

# Design and Analysis of 3D-MAPS: A Many-core 3D Processor with Stacked Memory

removed

## ABSTRACT

We describe the design and analysis of 3D-MAPS, a 64-core 3D stacked memory-on-processor, to be sent for fabrication using Tezzaron Semiconductor's 3D stacking technology. We also describe the design flow necessary to implement its layout using industrial 2D tools and in-house add-ons to handle through-silicon-vias (TSVs) and 3D stacking. We demonstrate the memory bandwidth advantage of 3D stacking that future many-core processors will require to meet their performance potential. Our 3D processor operates at 411MHz and achieves over 80GB/s memory bandwidth utilization on selected benchmarks.

## 1. INTRODUCTION

The potential of 3D IC stacking has been examined by researchers for many years. Only recently has the increasing cost of continuing process technology shrinks and the incredible memory-bandwidth demand of multi- and many-core systems brought 3D technology to the forefront of commercial interest. Several universities and companies are actively investigating and investing on 3D stacking technologies [2, 1]. One major challenge comes from the currently limited selection of industrial-grade EDA tools that support the design and analysis of 3D systems.

In this work we demonstrate our methodology for designing and analyzing 3D-MAPS (3D MASSively Parallel processor with Stacked memory), a 64-core 3D-stacked memory-on-processor system. For every step of the design process, we address the specific issues that 3D designers will encounter dealing with tools that are not specifically designed to meet their needs. There are several works presented in the literature that describe various 3D architecture design options and physical design algorithms for 3D ICs, but very few in the area of 3D design demonstration and methodology. Thorolfsson *et al.* [4] described the design of an FFT processor with 3D stacked memory implemented with MIT Lincoln Lab's 3-layer process [3]. However, they do not discuss cross-talk or power-noise analysis in 3D systems and do not

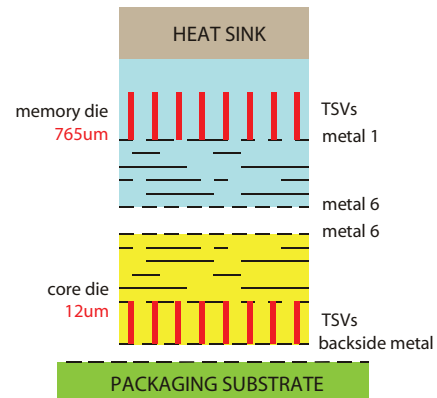


**Figure 1: Side view of the final stacked dies based on Tezzaron's F2F and TSV stacking technology**

include a thermal analysis. The contributions of this paper are as follows:

- This paper presents 3D-MAPS, arguably the first many-core 3D processor in academia. Our 3D processor contains 64 5-stage pipelined, 2-way in-order VLIW cores. Two dies are stacked in 3D-MAPS, one 64-core die and one SRAM die. Each core owns a dedicated 4KB SRAM tile, which is stacked above the core and connected using face-to-face 3D vias. Our architecture is verified with several multi-core benchmarks. 3D-MAPS demonstrates memory bandwidth of over 80GB/s based on our many-core benchmarks.
- This paper describes in detail how to construct the physical layouts of 3D-MAPS processor and how to perform various 3D analysis. Our tool-flow is based on commercial tools from Cadence, Mentor Graphics, and Synopsys and enhanced with various add-ons we developed to handle TSVs and 3D stacking. We provide sign-off 3D timing, power, thermal, IR-drop, signal integrity, and clock waveform analysis results based on DRC/LVS-passed 3D-GDSII layouts.

3D-MAPS is scheduled to be taped-out in January 2010 and fabricated using 130nm Chartered Technology and Tezzaron TSV/3D Technology. Once the fabrication and package/board design are completed in June 2010, our simulation results will be verified using various measurements.

## 2. 3D STACKING TECHNOLOGY

Permission to make digital or hard copies of all or part of this work for personal or classroom use is granted without fee provided that copies are not made or distributed for profit or commercial advantage and that copies bear this notice and the full citation on the first page. To copy otherwise, to republish, to post on servers or to redistribute to lists, requires prior specific permission and/or a fee.

Copyright 200X ACM X-XXXXX-XX-X/XX/XX ...\$10.00.

The 3D-MAPS processor will be fabricated using a six-metal 130nm process provided by Chartered Semiconductor that is modified to include through-silicon vias (TSVs) according to the specification of Tezzaron Semiconductor. The TSVs are manufactured in a via-first process. Trenches are dug into the silicon and filled with Tungsten. Then devices and metal layers are patterned. Next, wafers are flipped and bonded. Finally, one wafer is thinned until the trenched TSVs are revealed from the backside. This produces a two-layer face-to-face bonded stack that uses TSVs for IO. Because the wafers are bonded before thinning, there is never a need to handle a thinned wafer. Figure 1 shows a diagram of the completed die stack.

The Tezzaron process produces very small TSVs that are approximately  $1.2\mu\text{m}$  wide with  $2.5\mu\text{m}$  minimum pitch and  $6\mu\text{m}$  height. The face-to-face (F2F) connection, which is used for the main die-to-die communication, uses  $3.4\mu\text{m}$  Metal 6 pads with  $5\mu\text{m}$  pitch. The TSVs have a parasitic resistance of around  $600m\Omega$  and a parasitic capacitance of about  $15fF$ . The F2F connection has negligible resistance and capacitance, about the same as a local via. The 3D-MAPS die footprint is  $5 \times 5\text{mm}$ .<sup>1</sup> Therefore, the maximum face-to-face connection count is 1 million. The 130nm Chartered standard cell library provided to us includes only peripheral-style IO. For that reason, we include functional TSVs only underneath the IO-cell pads.<sup>2</sup> Dummy TSVs are inserted in the middle of the die to ensure that planarity requirements are met. More details on our F2F vias and TSVs are presented in Section 4.2 and Section 6.2.

### 3. 3D-MAPS ARCHITECTURE

#### 3.1 Core Architecture

The goal of our 3D-MAPS architecture is to demonstrate the rich bandwidth made possible by the high-density die-to-die vias when running data-parallel applications. Given that our design is area- and power-constrained, we also want to make cores and inter-core communication highly power-efficient [5], by eliminating unnecessary large, complex structures during the architectural planning stage.

Under this design philosophy, for the single core, we first defined a custom two-way VLIW architecture to eliminate area- and wire-dominated components such as complex decoder, dynamic instruction scheduler, reorder buffer, data disambiguation mechanism, etc. Instead, we offload these functionalities to the software side. In our two-way instruction format, one slot is dedicated to a memory instruction to consume memory bandwidth every cycle from the 3D-stacked memory while the other slot is tailored for an ALU instruction. When the memory instruction is absent, our ISA allows certain commonly used ALU instructions to be executed in the memory pipeline. To further keep memory bandwidth fully utilized by improving the memory-to-ALU instruction ratio, our ISA supports auto-increment.

On the other hand, to cope with control hazards without any impact on our limited area, we employed delay slots for change-of-flow instructions. Nonetheless, they are made completely transparent to the programmers as our assembler

will reschedule and ensure the correctness of the final binary. With assistance from the system software, the implementation can be relieved from those power- and area-consuming units such as branch predictor, branch target buffer, and pipeline squashing mechanism for mis-speculation while maintaining similar execution efficiency of being speculative.

One major drawback of a VLIW architecture is the potentially enlarged code size due much to software’s incapability of finding useful instructions to fill in the gaps created by instruction dependence or delay slots. To address this issue, we proposed a low-cost compression scheme at the instruction encoding level by allocating two prefix bits to indicate the number of NOP pairs followed by the current instruction. For our benchmark programs, we were able to reduce NOPs by 14% to 57%.

The design of inter-core communication in a many-core processor can lead to numerous implications for power, performance, and even routing space. Again, to minimize power consumed by the interconnect, we employed a point-to-point 2D mesh communication paradigm controlled by explicit communication and synchronization instructions. In particular, we found a 2D mesh network addresses some issues of the two other alternatives: 2D torus and folded-torus network topology. First, a simple 2D mesh eliminates the long wires that connect two cores on the boundaries of the same row or column in a 2D torus. Second, it halves the wire routing space required over the core-to-core boundary of a folded torus. Although such an explicit communication model could reduce programmers’ productivity, it can provide higher performance, yet reduce dynamic power at the same time. In particular, we argue that a network-on-chip router would be overkill, since most of the data-parallel applications demonstrate stable, predictable, and regular communication patterns among cores when properly partitioned. Each of our 3D-MAPS cores features four buffers for sending or receiving data from its north, south, east, or west neighbor. Synchronization among cores is achieved by a global barrier, whose implementation was laid out as an H-tree on the core layer.

#### 3.2 Architecture Verification

In the verification process, we developed a multi-level framework to rigorously verify each stage of the design. Our baseline reference models are simply those output generated by an x86 machine running our benchmark written in high-level language. We then rewrote the benchmark using pseudo-assembly language at register-transfer level in C, *e.g.*, declaring an array of variables to emulate the register file of our architecture, and test the benchmark on an x86 machine. Our pseudo-assembly codes were then ported using our 3D-MAPS ISA, assembled and optimized by our assembler, and simulated on our architectural simulator. The simulation output was verified at cycle-level in lock-step with that of the pseudo-assembly reference model. Up to this point, we have an architectural simulator that conforms to correct functional behavior and predicts the performance of the benchmarks for 3D-MAPS. Finally, we verify the RTL design against our architectural simulator using pipeline traces.

#### 3.3 Off-chip Interface

The primary design goal for the off-chip interface was to minimize the pin count. Therefore, the interface was modeled after the IEEE 1149.1 test access port with two key

<sup>1</sup>This is the space assigned to us as part of the 2009 DARPA/Tezzaron multi-project wafer run.

<sup>2</sup>Future 3D-MAPS processors will employ “true” 3D cores, where modules and/or gates are spread into multiple dies.

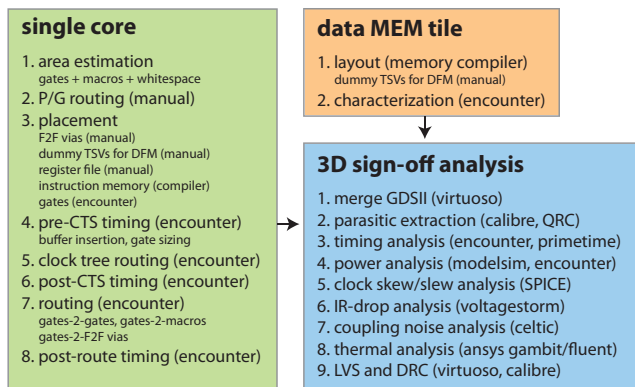


**Figure 2: Our flow for the design and analysis of single core and single memory tile stack.**

deviations. First, we use a custom *test control state machine* (TCSM), which has complete control of the chip, managing functional test, memory loading, and program execution. Second, we have four pairs of *test data in* and *test data out* (TDI and TDO) pins, instead of the standard one pair. Internally, the sixty-four cores are grouped into four groups of sixteen cores each. The chains in each bank connect serially to one pair of I/O pins. This grouped design allows the chip to fail gracefully; a failure can, at most, only disable a single group. There are, of course, some failures that would be catastrophic (e.g. a failure in the TCSM), but the number of such failures is negligible compared to the number of recoverable failures.

## 4. PHYSICAL DESIGN METHODOLOGY

Figure 2 shows the overall physical design flow used to produce single core plus single memory tile layouts in 3D-MAPS. The physical design flow begins with an RTL description of the processor core written in VHDL. Our top-level module contains single core (bottom-die), 4 data memory banks (top), 1 instruction memory bank (bottom), and custom-designed register file (bottom). We then use Synopsys Design Compiler to compile VHDL into structural Verilog for each die. The compiled Verilog is then input into Cadence Encounter to perform the automated physical design steps. We use Cadence Encounter to perform gate placement, sizing and buffering optimization, signal routing, clock routing, and power and ground network generation. We also use many of the tools integrated into Encounter to perform early analysis on the design to ensure reasonableness before sign-off analysis is undertaken. However, Cadence Encounter and its integrated point-tools do not understand F2F vias, TSVs, and 3D stacking, i.e., multiple die definitions. Thus, we have developed several add-ons and found ways to manipulate LEF/DEF and other intermediate files to manage F2F vias, TSV, and 3D stacking. The instruction and data memory bank, tile, and die designs are done with a memory compiler provided by Artisan.

### 4.1 3D Power Ground Network Generation

The power and ground distribution networks are generated mainly using the stripe and ring generation commands in Cadence Encounter. The goal is to have the rings on both the core layer and memory layer line up. By lining up these rings we can connect them using the vast array of face-to-face (F2F) connections. This allows the creation of a very

low resistance connection for the power and ground distribution to the memory layer. Decoupling capacitors (decaps) are inserted into the design using Cadence Encounter. This is done prior to placement to provide an even distribution of capacitance. In the memory layer, we insert a large amount of decaps on the power rings in the blank space around the memory banks. This allows the memory layer to provide large amounts of on-demand current to the cores.

### 4.2 F2F Via and TSV Placement

Communication between the core and memory dies occurs through the face-to-face (F2F) vias as shown in Figure 1. Any net that connects to a F2F via, and thus circuitry on the other die, is called a 3D net. The individual design for each wafer therefore must contain pins for all nets that cross the F2F boundary. The memory layer contains only the data memory banks and their connections. Accordingly, we first fix the location of the memory banks, then we manually place pins in both dies directly above the pins on the memory banks. The TSVs are used only for off-chip IO in our current version of 3D-MAPS. The foundry-supplied IO cell library is peripheral-style only. Therefore, the only electrically active TSVs are placed inside the IO cells underneath the bond-pad.

One unique requirement Tezzaron TSV process imposes is on mandatory TSV pitch of  $250\mu m$  throughout the entire wafer. Thus, there needs to be at least one TSV inside a  $250\mu m$  window. This requirement is to maintain the planarity of the wafer during chemical and mechanical polishing (CMP). Because the 3D-MAPS cores are  $560 \times 560\mu m$  and we do not use TSVs inside the core region, we must place a  $3 \times 3$  array of dummy TSVs inside each core to meet this maximum pitch requirement. We manually inserted these dummy TSVs before placement as shown in Figure 3(e).

### 4.3 3D Placement and Routing

Cadence Encounter is used to perform placement and routing at both the many-core level and the single-core level. The 3D connection information is propagated to the placer through the use of fixed pins on Metal 6 representing the F2F connections. These pins constrain the placement to optimize correctly for the full 3D system.

Cadence Encounter is also used to perform sizing and buffering optimizations, and NanoRoute is used to perform routing. The 3D connection information is propagated to the optimizer and router through back-annotation of capacitance and arrival time requirements on the fixed pins. These constraints force the optimization engine and the router to account correctly for both sides of the 3D nets.

### 4.4 3D Clock Routing

We perform clock routing using the clock tree synthesis functions of Cadence Encounter. The clock network is contained mainly within the core layer. Each memory bank in the memory layer has a clock pin that is propagated to the core layer using a fixed F2F connection. This pin is annotated with the capacitance of the routing inside the memory layer as well as the gate capacitance of the clock pin on the memory bank itself. This minimizes the clock skew for both the single core and memory tile stack. At the many-core level, each core has a single input clock pin.

## 5. 3D SIGN-OFF ANALYSIS

The existing Cadence, Synopsys, and Mentor Graphics tools are designed for 2D ICs and do not handle 3D designs and TSVs. The following sections describe our strategy to extend these tools to analyze and verify 3D-MAPS.

### 5.1 3D Timing and Signal Integrity Analysis

Our 3D timing analysis is based on Synopsys PrimeTime. First, we prepare the Verilog netlist files of both dies and the SPEF files containing extracted parasitic values for all the nets of the dies. Then, we create a top-level Verilog netlist that instantiates the design of each die and connects the 3D nets using F2F connections. We also create an SPEF file that has a parasitic model of the F2F connections. After that, we run PrimeTime with all the Verilog files and the SPEF files to get the timing analysis results.

3D signal integrity analysis must also contain a 3D component because nets may have enough coupling capacitance to be considered a problem only when all dies are considered simultaneously. For signal integrity analysis, we use Cadence CeltIC. Again, we input an SPEF file that contains the information for both dies and the parasitics from the F2F connections. Then with the merged Verilog netlist, CeltIC finds all the paths with noise violations.

### 5.2 3D Power Noise Analysis

We perform 3D power noise analysis using Cadence VoltageStorm. The stand-alone VoltageStorm takes in a DEF file, technology files, and power dissipation files to generate both peak and average power noise values. Performing this analysis for a 3D design is a challenge.

For our design, we perform true 3D power noise analysis with VoltageStorm. To accomplish this, we compile a technology file that contains all of the 3D layers. This technology file contains multiple copies of each metal layer, one for each layer in the 3D stack. Then, 3D DEF files are constructed from the design of each layer. A separate LEF file must also be constructed that contains instances specific to each layer. Finally, this information is fed into VoltageStorm to obtain true 3D power noise values.

### 5.3 3D Thermal Analysis

3D designs have the potential to suffer from significant thermal problems due to the higher thermal resistance between active silicon layers and the heatsink. We use ANSYS Gambit and Fluent for our thermal analysis. Gambit is a meshing and model generation software that sets up thermal analysis problems. Fluent is the simulation engine that calculates the thermal distribution of the chip.

Gambit is used to model the 3D chip-stack and includes both core and memory layers, as well as a model of the rest of the package and a 5mm tall heatsink. The stack is first divided into numerous thermal layers such as gates, poly, Metals 1-6, via, dielectric, *etc.* To determine the material properties for each mesh volume, the GDSII file is parsed to determine the correct ratio between the various materials of each layer at each particular grid point.

This ratio is used to calculate the weighted average of the material properties and to determine the effective thermal conductivity of that grid point. Power sources are then inserted into each mesh volume. Finally, Fluent is used to calculate the steady-state thermal map.

**Table 1: Architectural performance metrics.**

Benchmark	Memory Bandwidth (GB/s)	IPC	BIPS
string_search	18.4	0.65	17.10
matrix_multiply	1.5	0.32	8.42
median	84.5	1.62	42.61
aes_encrypt	53.4	0.97	25.51
space 1	<b>COMING UP?</b>	<b>COMING UP?</b>	<b>COMING UP?</b>
space 2			

## 6. LAYOUT AND ANALYSIS RESULTS

### 6.1 Architectural Simulation Results

Table 1 shows the results from our many-core architectural simulations of the 3D-MAPS processor. The table reports memory bandwidth in gigabytes per second (GB/s), instructions per cycle (IPC), and billions of instructions per second (BIPS). In general, 3D-MAPS achieves memory bandwidth around 40 GB/s, which is comparable to the memory bandwidth used by a typical graphics processor.

### 6.2 Physical Layouts

Figure 3(a-c) show various layout views of the 3D-MAPS processor. The core footprint is  $560 \times 560 \mu m$ . The layout of one tile of SRAM memory is also shown. A single tile contains 4 banks of 1KB data memory. Thus, the total SRAM data memory capacity of 3D-MAPS processor is  $4KB \times 64 = 256KB$ . The full many-core layout of the core layer has dimension of  $5 \times 5mm$ . Each core is arrayed in an  $8 \times 8$  grid and core-to-core communication occurs using short wires. The core-to-core pitch is  $570 \mu m$  in both the  $x$  and  $y$  directions. The pitch of the memory tiles matches that of the cores,  $570 \mu m$ .

Figure 3(d) shows the F2F connections used for the 3D communication (purple) and power and ground network distribution (red and green). The nets connected to the F2F communication pads are highlighted in blue. There are 1,018 power and ground F2F connections per core, and 65,152 power and ground F2F connections over the entire die. Each core also uses 116 F2F connections for signals and clock, for a total of 7,424 F2F connections over the entire die. Figure 3(e) denotes the location of the TSVs in the core layer. The dummy TSVs, shown in navy, are located inside the cores.<sup>3</sup> The IO TSVs, shown in red, are located around the periphery. There are 1,784 TSVs used for IO and 576 dummy TSVs. Timing optimization inserted 970 buffers into each of the cores. The buffer distribution is shown in Figure 3(f).

### 6.3 3D Sign-off Analysis Results

The 3D IR drop inside a single core is shown in Figure 4(a). The supply voltage for 3D-MAPS set to 1.5V. The total drop is about  $13mV$  inside one core. The IR drop inside a single memory tile is shown in Figure 4(b). The total drop is about  $10mV$ . These values include true 3D-aware IR-drop analysis using sign-off-level Cadence VoltageStorm software.

3D timing analysis reports that the 3D-MAPS processor is capable of running at  $411MHz$ . The timing critical path inside each core is shown in Figure 4(c). The timing critical path runs through several muxes and the multiplier. The longest delay for a 3D net is for the address bus, which

<sup>3</sup>These dummy TSVs are enlarged for visibility.



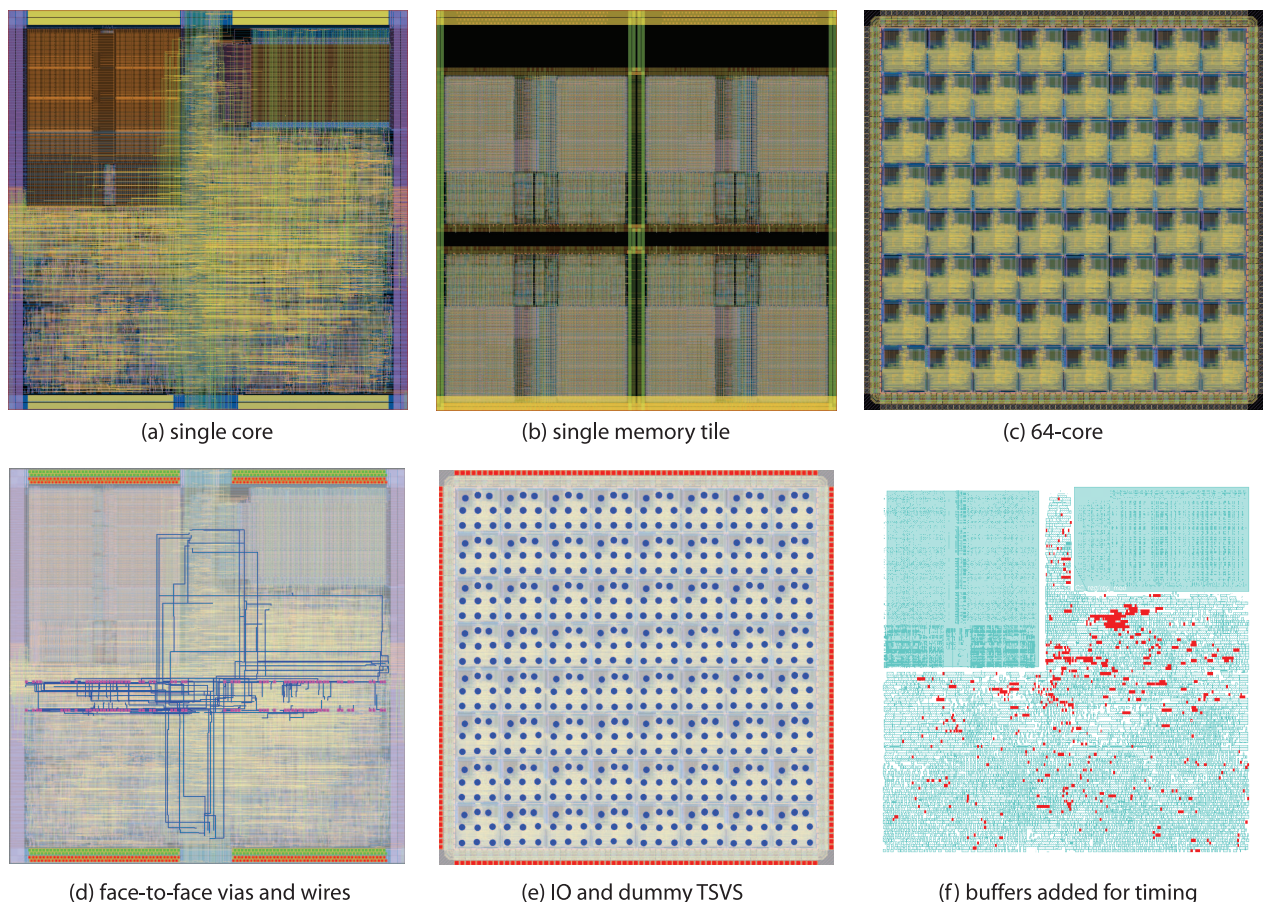


**Figure 3: Various layout views of the 3D-MAPS processor.**

has a sink in each of the four memory banks and thus has larger wirelength. The 3D timing critical path is shown in Figure 4(d) and (e). Figure 4(f) shows the top 5 3D nets that experience the most switching noise inside each core. The maximum noise value on the worst net is  $674mV$ , which is very close to the noise limit. The next highest noise value is much lower at  $592mV$ . There are a few 2D nets that experience more noise than the noisiest 3D nets.

The power map for a single core simulated using the string-search benchmark is shown in Figure 4(g). The figure shows that the instruction memory consumes the largest amount of power. The single core thermal map is shown in Figure 4(h). The temperature is highest near the West side of the core. The maximum temperature is approximately  $47^{\circ}C$ . The 64-core thermal map is shown in Figure 4(i).

Figure 4(j) and (k) show the clock distribution nets at the single- and 64-core levels, respectively. The clock signal skew at the multi-core level (between two core's clock input pins) is  $45.3ps$ . The skew between the flip-flops inside a single core is  $22.7ps$ . Therefore, the total flip-flop to flip-flop skew over the entire design is  $68.0ps$ . The slew for the clock signals is around  $117ps$  for both rise and fall.

Figure 4(l) shows HSPICE simulations for the clock tree. The first waveform shows the sine wave input from the off-chip PLL at the IO voltage. The second waveform shows the output of the input buffer cell that converts the IO voltage sine wave to the square core-voltage clock signal. The third waveform displays the output of the clock drivers that drive the input buffer's square signal to the clock distribution net-

work. The final two waveforms show the clock signal at the input to the cores and then the flip-flops inside the cores.

## 7. CONCLUSIONS

We have presented the design and analysis methodology used to produce 3D-MAPS, a 64-core memory on processor 3D stacked system, to be fabricated using a  $130nm$  process with via-first TSVs. We produced the layouts using commercially-available tools with several custom add-ons to enable full 3D design and analysis. The 3D-MAPS design simulates correctly at  $411MHz$  and achieves a memory bandwidth above  $80GB/s$  on selected benchmarks.

## 8. REFERENCES

- [1] X. Dong and Y. Xie. System-level cost analysis and design exploration for 3d ics. In *Proc. Asia and South Pacific Design Automation Conf.*, 2009.
- [2] M. Koyanagi, T. Fukushima, and T. Tanaka. Three-dimensional integration technology and integrated systems. In *Proc. Asia and South Pacific Design Automation Conf.*, 2009.
- [3] Massachusetts Institute of Technology Lincoln Labs. *MITLL Low-Power FDSOI CMOS Process Design Guide*. revision 2008:6 edition. September 2008.
- [4] T. Thorolfsson, K. Gonsalves, and P. Franzon. Design automation for a 3dic fft processor for synthetic aperture radar: A case study. In *Proc. ACM Design Automation Conf.*, pages 51–56, 2009.
- [5] D. H. Woo and H.-H. S. Lee. Extending Amdahl's Law for Energy-Efficient Computing in the Many-Core Era. *IEEE Computer*, 41(12):24–31, 2008.



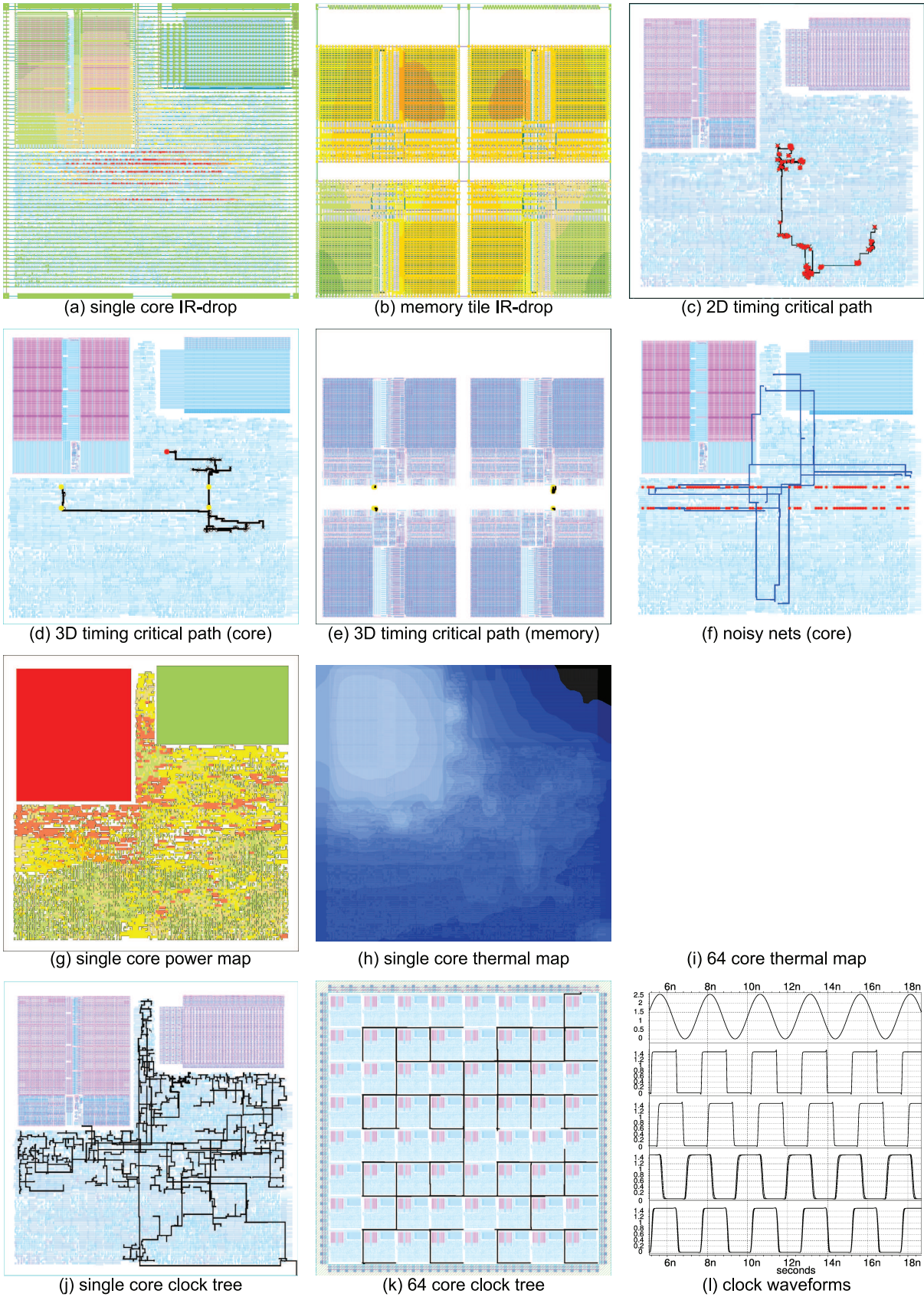


Figure 4: Various 3D sign-off analysis results for the 3D MAPS processor.